

Positive2Negative: Breaking the Information-Lossy Barrier in Self-Supervised Single Image Denoising

Tong Li¹ Lizhi Wang^{2*} Zhiyuan Xu¹ Lin Zhu¹ Wanxuan Lu³ Hua Huang²
¹Beijing Institute of Technology ² Beijing Normal University ³ Chinese Academy of Sciences

Abstract

Image denoising enhances image quality, serving as a foundational technique across various computational photography applications. The obstacle to clean image acquisition in real scenarios necessitates the development of self-supervised image denoising methods only depending on noisy images, especially a single noisy image. Existing self-supervised image denoising paradigms (Noise2Noise and Noise2Void) rely heavily on information-lossy operations, such as downsampling and masking, culminating in low quality denoising performance. In this paper, we propose a novel self-supervised single image denoising paradigm, Positive2Negative, to break the information-lossy barrier. Our paradigm involves two key steps: Renoised Data Construction (RDC) and Denoised Consistency Supervision (DCS). RDC renoises the predicted denoised image by the predicted noise to construct multiple noisy images, preserving all the information of the original image. DCS ensures consistency across the multiple denoised images, supervising the network to learn robust denoising. Our Positive2Negative paradigm achieves state-of-the-art performance in self-supervised single image denoising with significant speed improvements. The code will be released to the public.

1. Introduction

Image denoising plays a vital role in image processing to enhance visual quality [12], serving as a foundational technique across various computational photography applications [3, 36]. The widespread popularity of paired clean-noisy image datasets [1, 32] has catalyzed advancements in supervised methods, yielding remarkable performance [7, 48]. However, supervised methods fall short in dynamic scenes [16, 20], where long exposure results in misalignment and blur [20, 39], hindering the acquisition of clean images. Therefore, advancing self-supervised image denoising methods using only noisy images [23, 40], espe-

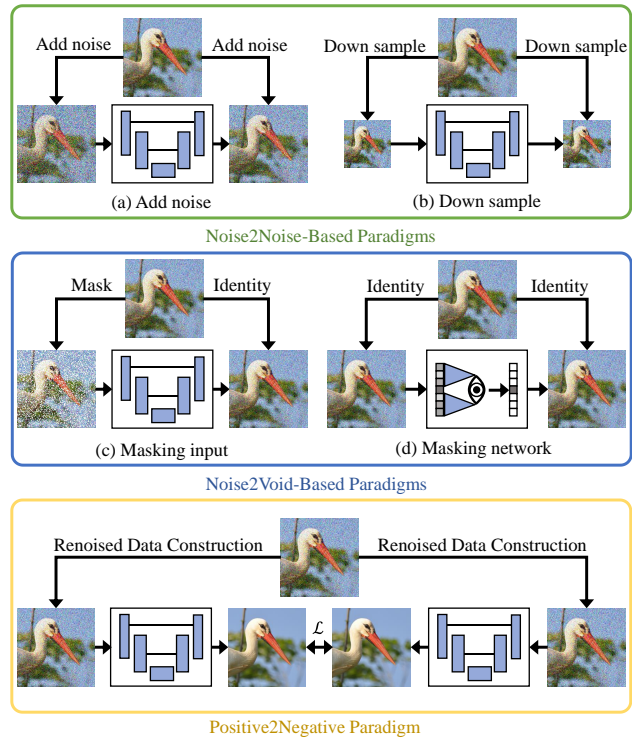


Figure 1. **Information-lossy operations in current paradigms.** The noise addition operation reduces the signal-to-noise ratio, the downsampling operation lowers the sampling density, and the masking operation neglects crucial central pixels. Each of these operations introduces an information-lossy barrier [8, 29, 34], culminating in imprecise denoising.

cially a single noisy image [9, 11, 22, 25], holds significant importance.

The crux of self-supervised image denoising methods lies in the construction of the training data and the formulation of the supervision strategy. Current methods are divided into Noise2Noise-based paradigms and Noise2Void-based paradigms, as illustrated in Figure 1. Noise2Noise-based paradigms add additional noise to the noisy image [26, 31] or down sample the noisy image [13, 25] to approximately construct two independently noisy observations as training data. These paradigms learn denoising by

*Corresponding Author: Lizhi Wang (wanglizhi@bnu.edu.cn)

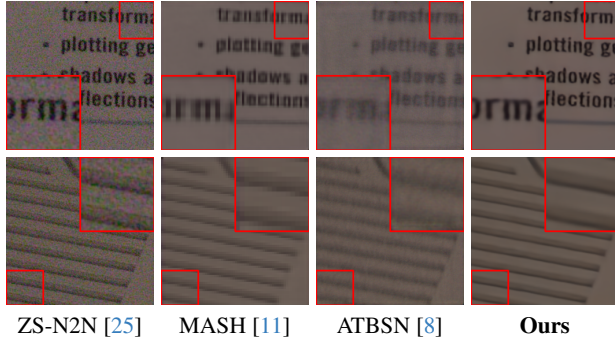


Figure 2. **The information-lossy barrier significantly compromises the image quality.** The information-lossy operations construct imprecise training data and the model only learns imprecise denoising [8, 30, 34, 38], resulting in remaining noise (as shown by the results of ZS-N2N), aliasing effects (as shown by the results of MASH) and texture loss in denoised images (as shown by the results of ATBSN).

supervising the denoised result of one observation with the other observation. Noise2Void-based paradigms mask the noisy image [16, 37] or the neural network [8, 19, 38] to construct masked training data. These paradigms learn denoising by supervising the denoised result of the masked central pixel with the original noisy pixel, where the prediction only relies on the surrounding pixels.

However, existing methods rely heavily on information-lossy operations, culminating in low quality denoising performance [19, 30, 37, 38]. Specifically, the noise addition operation reduces the signal-to-noise ratio, the down-sampling operation lowers the sampling density and the masking operation neglects crucial central pixels. Each of these operations loses the information from the original noisy image [8, 29, 34], inevitably compromising the denoising ability [38, 41]. Consequently, denoised images always suffer from remaining noise, aliasing effects or texture loss [42, 43], as shown in Figure 2. As these information-lossy operations constitute the indispensable foundation of the Noise2Noise-based and Noise2Void-based paradigms, it is imperative to establish a new paradigm that transcends the Noise2Noise-based and Noise2Void-based paradigms.

In this paper, we propose a new self-supervised single image denoising paradigm, Positive2Negative, to break the information-lossy barrier. Our inspiration stems from the observation that noise distributions are approximately symmetrical and centered around zero, implying that the opposite noise also follows the distribution of the original noise. Leveraging this insight, we can construct multiple noisy images corresponding to the same clean image, which serves as the basis of Positive2Negative. Concretely, Positive2Negative relies on two steps: Renoised Data Construction (RDC) and Denoised Consistency Supervision (DCS).

The basic idea of RDC is to construct training data.

Specifically, we design a zero-mean sampling strategy to construct multi-scale Positive noise and Negative noise based on the predicted noise, which are then added back to construct Positive noisy images and Negative noisy images. The constructed data covers all the information of the given single image, thus the Positive2Negative paradigm breaks the information-lossy barrier.

The basic idea of DCS is to formulate a supervision strategy. Specifically, given the constructed multi-scale noisy images, DCS supervises the network to generate consistent denoised outputs during the training process. Furthermore, we provide a theoretical analysis showing that the Positive2Negative paradigm can learn robust denoising, through supervising the multiple denoised images.

In summary, our contributions are as follows:

- We propose a new self-supervised single image denoising paradigm, Positive2Negative, to break the information-lossy barrier.
- We propose a data construction method, which constructs multi-scale similar noisy images for training.
- We propose a denoising supervision method, which is theoretically guaranteed to learn robust denoising.
- Positive2Negative achieves SOTA performance over self-supervised single image denoising, with significant speed improvements.

2. Related Work

From the training data perspective, the self-supervised image denoising methods can be classified into noisy dataset based methods and single image based methods.

2.1. Noisy Dataset based Methods

Noisy dataset based methods represent the most active research direction in image denoising. These methods learn to denoise from a given noisy dataset. Generally, a larger volume of the noisy dataset improves the denoising performance. As a result, in scenarios where only a single noisy image is available, the denoising performance of whole noisy dataset-based methods decreases significantly.

Noise2Noise [20] learns denoising by mapping one noisy observation to another independent observation of the same scene. Subsequent studies focus on generating observations of the same scene from a single observation, typically achieved through downsampling [13, 25] or by introducing additional noise [26, 31, 47, 51, 55]. After that, another elegant method Noise2Void [16] is proposed. Noise2Void [16] assumes that the noise distribution is zero-mean, the noise is spatially independent, and the signal is spatially correlated. Noise2Void [16] predicts the clean signal by leveraging surrounding noisy signals, with masking the central pixel. Various other works propose alternative masking schemes [2, 17, 18, 37, 45, 49]. Noise2Void

struggles with real-world noise, which often exhibits spatial correlation. Therefore, subsequent research endeavors to break the noise spatial correlation [8, 19, 21, 38, 44, 54]. Additionally, some methods amalgamate aspects from both Noise2Noise and Noise2Void approaches [14, 30]. Moreover, several methodologies [5, 15, 28, 53] have transcended the frameworks established by Noise2Noise and Noise2Void. For instance, CVF-SID [28] employs cycle consistency principles, while LUD-VAE [53] introduces a degradation modeling method.

Noisy dataset based methods have high requirements for the volume of training data and fail in scenarios where only a single noisy image is available [9, 11].

2.2. Single Image based Methods

Single image based methods represent the most challenging situation for denoising and the least demanding requirements for data. These methods learn to denoise from a given single noisy image without any dependence on paired noisy-clean or noisy datasets. As a result, single image based methods are less developed due to the inherent difficulty, only gaining attention in the past two years.

DIP [35] is the earliest self-supervised image denoising method. DIP [35] learns to map random noise to a given noisy image and employs early stopping to prevent overfitting. Self2Self [33] uses dropout to create two Bernoulli-sampled observations of a noisy image and learns to map one sampled noisy image to another. R2R [31] is a kind of Noise2Noise-based method and constructs two independent samples from a single noisy image by adding extra noise. ScoreDVI [9] performs real denoising using a pre-trained Gaussian denoiser and an estimated noise model. ZS-N2N [25] extend Noise2Noise [20] to a single image version by downsampling. MASH [11] is a kind of Noise2Void-based method, employing masking and local pixel shuffling to break the noise spatial correlation.

In this paper, we propose Positive2Negative, a new self-supervised single image denoising paradigm, to break the information-lossy barrier.

3. Positive2Negative

In this section, we first demonstrate the motivation of Positive2Negative in Section 3.1. After that, we present the two critical steps of Positive2Negative: RDC and DCS, respectively in Section 3.2 and Section 3.3. Finally, we provide an analysis and proof of Positive2Negative in Section 3.4.

3.1. Motivation

Our inspiration stems from the widely recognized assumptions that the noise distribution is zero-mean and approximately symmetrical [16, 20], which is consistent with our observation. In our observation experiment, we calculate

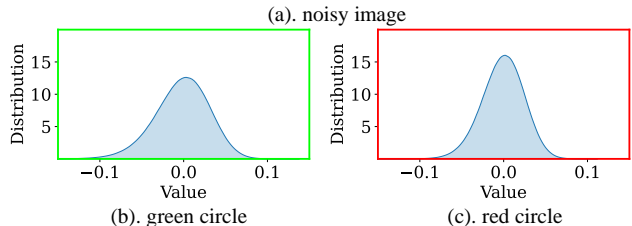
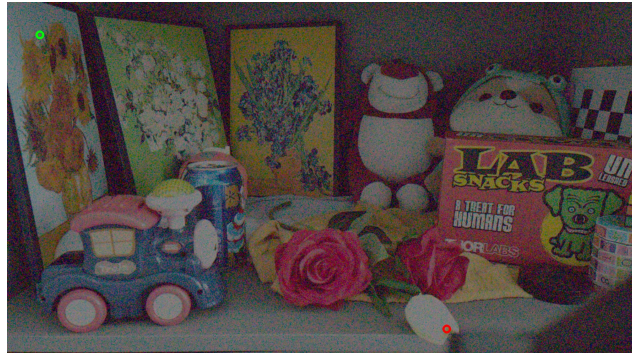


Figure 3. **Noise distribution is zero-mean and approximately symmetrical.** (a) shows a noisy image. (b) and (c) show the noise distributions, which are calculated at the center pixels marked by the green circle and the red circle in the noisy image, respectively. It is obvious that the noise distribution is zero-mean and approximately symmetrical.

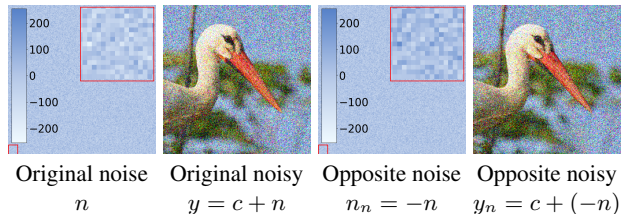


Figure 4. The opposite noise $-n$ is similar to the original noise n . The opposite noise $-n$ approximately follows the original noise’s distribution, which is zero-mean and approximately symmetrical.

the noise distribution of a fixed pixel across multiple observations of the same scene. As shown in Figure 3, the noise distribution is zero-mean and approximately symmetrical. (More analysis about the noise distribution can be found in the supplementary materials.) Based on this observation, an intuitive idea is that the opposite noise $-n$ also follows the same distribution as that of the original noise n . This intuitive idea inspires us to construct the opposite noise n_n and corresponding opposite noisy image y_n :

$$n_n = -n, \quad (1)$$

$$y_n = x + n_n = x - n. \quad (2)$$

The opposite noise n_n and opposite noisy image y_n are similar to the original noise n and original noisy image y , respectively, as shown in Figure 4.

Based on the above observations and insights, we propose the Positive2Negative paradigm, as shown in Figure 5.

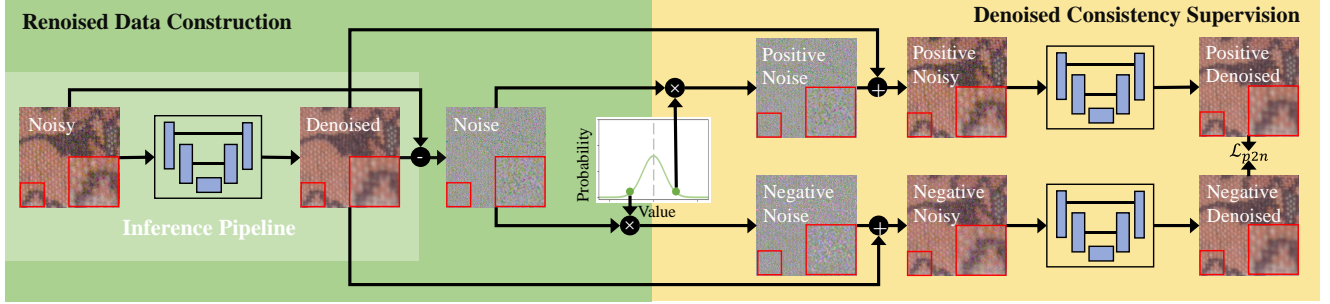


Figure 5. **Overview of the proposed self-supervised single image denoising paradigm.** For training, the Positive2Negative paradigm consists of 2 steps. The first step is Renoised Data Construction (RDC): multiply the predicted noise by positive and negative coefficients to construct multi-scale Positive noise and Negative noise, respectively. The second step is Denoised Consistency Supervision (DCS): train the network through supervising the consistency of the denoised images. For inference, denoising can be achieved in just one pass through the network. (The networks shown in the figure are the same one. In addition, for better visualization, the images within the red boxes on the bottom left have been zoomed in and are displayed in the red boxes on the bottom right.)

Firstly, we extend our intuitive idea into a flexible and up-graded version: Renoised Data Construction (RDC), which constructs multiple positive and negative noises. This improvement also eliminates the need for the symmetrical nature of the previous intuitive idea. Secondly, we propose the Denoised Consistency Supervision (DCS), which supervises the consistency of the predicted denoised images to learn a denoising neural network. DCS is theoretically guaranteed.

It is important to note that we do not require the noise distribution to be strictly zero-mean or symmetric. Although real noise generally has a zero-mean, certain cases where this assumption is not strictly met can be easily addressed by adjusting the norm in the loss function [20].

3.2. Renoised Data Construction (RDC)

The basic idea of RDC is to denoise the image to predict a denoised image and renoise the predicted denoised image by the predicted noise to construct multiple noisy images.

For a given noisy image $y = x + n$, where x presents the clean image and n presents the noise. RDC firstly denoises the noisy image y once through the neural network \mathcal{F} parametered by θ :

$$\hat{x} = \mathcal{F}_\theta(y). \quad (3)$$

Here \hat{x} is the predicted denoised image of the noisy observation y . Then we can calculate the predicted noise \hat{n} within the noisy observation y :

$$\hat{n} = y - \hat{x}. \quad (4)$$

Next, RDC constructs noisy images as training data based on the predicted noise \hat{n} and the predicted denoised image \hat{x} . As noise is zero-mean, we further design a zero-mean sampling strategy to construct new noises. Specifically, RDC multiplies the predicted noise \hat{n} by both positive scale parameters σ_p and negative scale parameters $-\sigma_n$

sampled from Gaussian distribution \mathcal{N} , constructing multi-scale Positive noise n_p and Negative noise n_n , respectively:

$$\sigma_n, \sigma_p \sim \mathcal{N}(1, \sigma) \quad (5)$$

$$n_p = \sigma_n \hat{n}, \quad (6)$$

$$y_p = \hat{x} + n_p = \hat{x} + \sigma_n \hat{n}, \quad (7)$$

$$n_n = -\sigma_p \hat{n}, \quad (8)$$

$$y_n = \hat{x} + n_n = \hat{x} - \sigma_p \hat{n}. \quad (9)$$

3.3. Denoised Consistency Supervision (DCS)

The basic idea of DCS is that the noisy observations y_p and y_n should correspond to the same clean image. Therefore, the loss supervises the consistency of the predicted denoised images:

$$\mathcal{L}_{p2n} = \|\mathcal{F}_\theta(y_p) - \mathcal{F}_\theta(y_n)\|, \quad (10)$$

where $\|\cdot\|$ represents the norm. The norm should be selected based on the characteristics of the noise distribution to effectively handle different distributions. Considering the general nature of noise [20], we employ a gradually varying norm function $\|\cdot\|_{2 \rightarrow 1.5}$ to cover a broader range of unknown distributions:

$$\|x\|_{2 \rightarrow 1.5} = (|x| + \epsilon)^\gamma, \quad (11)$$

where $\epsilon = 10^{-8}$ and γ varies linearly from 2 to 1.5 during training. The advantage of the varying $\|\cdot\|_{2 \rightarrow 1.5}$ norm is that $\|\cdot\|_{2 \rightarrow 1.5}$ does not require fine-tuning of parameters, yet $\|\cdot\|_{2 \rightarrow 1.5}$ consistently delivers robust performance.

The noisy observations y_p and y_n contain multi-scale noise. Through DCS, the neural network \mathcal{F}_θ gradually learns to become insensitive to input noise and consistently outputs the clean signal, achieving the desired denoising performance.

Table 1. **Quantitative comparisons** on SIDD, CC, PolyU and FMDD datasets. The best and second-best results (PSNR \uparrow / SSIM \uparrow) are marked in **red** and **blue** in self-supervised single image denoising methods. The results of noisy dataset based self-supervised methods and supervised methods are also provided, only as a reference comparison. More evaluation details of each method can be found in the supplementary materials. SIDD val and SIDD ben represent the SIDD validation dataset and the SIDD online benchmark, respectively.

Category	Method	SIDD val [1]	SIDD ben [1]	CC [27]	PolyU [46]	FMDD [50]
Supervised	Unprocessing [4]	28.12 / 0.529	31.64 / 0.531	35.18 / 0.908	36.99 / 0.970	28.45 / 0.574
	MaskedDenoising [6]	28.67 / 0.604	31.99 / 0.601	33.87 / 0.930	34.56 / 0.955	29.86 / 0.646
	CLIPDenoising [10]	34.79 / 0.866	35.82 / 0.859	36.30 / 0.941	37.54 / 0.979	30.56 / 0.708
Self-Supervised (Noisy Dataset Based Methods)	Noise2Void [16]	29.35 / 0.651	27.68 / 0.668	32.27 / 0.862	33.83 / 0.873	-
	CVF-SID [28]	34.81 / 0.944	35.05 / 0.856	33.29 / 0.913	35.86 / 0.937	32.73 / 0.843
	LUD-VAE [53]	34.91 / 0.892	35.49 / 0.883	35.48 / 0.941	36.99 / 0.955	-
Self-Supervised (Single Image Based Methods)	DIP [35]	32.11 / 0.740	-	35.61 / 0.912	37.17 / 0.912	32.90 / 0.854
	PD-denoising [54]	33.97 / 0.820	-	35.85 / 0.923	37.04 / 0.940	33.01 / 0.856
	NN+denoiser [52]	-	-	36.52 / 0.943	37.66 / 0.956	32.21 / 0.831
	Self2Self [33]	29.46 / 0.595	29.51 / 0.651	37.44 / 0.948	37.52 / 0.951	30.76 / 0.695
	R2R [31]	24.59 / 0.526	-	33.43 / 0.956	36.23 / 0.956	27.17 / 0.525
	APBSN-single [19]	30.90 / 0.818	-	27.72 / 0.891	29.61 / 0.897	28.43 / 0.804
	ScoreDVI [9]	34.75 / 0.856	35.39 / 0.859	37.09 / 0.945	37.77 / 0.959	33.10 / 0.865
	ZS-N2N [25]	25.59 / 0.565	30.19 / 0.428	33.51 / 0.957	35.99 / 0.959	31.65 / 0.767
	MASH [11]	35.06 / 0.851	34.80 / 0.814	31.17 / 0.954	37.62 / 0.932	33.71 / 0.882
	ATBSN-single [8]	32.39 / 0.865	27.86 / 0.312	31.87 / 0.962	33.21 / 0.960	31.23 / 0.829
	Positive2Negative	35.24 / 0.928	35.80 / 0.875	37.92 / 0.987	38.20 / 0.988	34.00 / 0.887

3.4. Analysis

In this section, we provide an analysis and proof demonstrating how the Positive2Negative paradigm achieves denoising.

Taking the 2-norm as an example, the loss function can be expressed as:

$$\mathcal{L}_{p2n} = \mathbb{E} [\|\mathcal{F}_\theta(y_p) - \mathcal{F}_\theta(y_n)\|^2]. \quad (12)$$

Through Taylor expansion, we can approximate the predicted denoised images $\mathcal{F}_\theta(y_p)$ and $\mathcal{F}_\theta(y_n)$:

$$\mathcal{F}_\theta(y_p) = \mathcal{F}_\theta(\mathcal{F}_\theta(y)) + \sigma_p \cdot \frac{\partial \mathcal{F}_\theta(y)}{\partial y} \cdot n + \mathcal{O}(n^2), \quad (13)$$

$$\mathcal{F}_\theta(y_n) = \mathcal{F}_\theta(\mathcal{F}_\theta(y)) - \sigma_n \cdot \frac{\partial \mathcal{F}_\theta(y)}{\partial y} \cdot n + \mathcal{O}(n^2). \quad (14)$$

Substituting the approximations, we get:

$$\mathcal{F}_\theta(y_p) - \mathcal{F}_\theta(y_n) \approx (\sigma_p + \sigma_n) \cdot \frac{\partial \mathcal{F}_\theta(y)}{\partial y} \cdot n. \quad (15)$$

With further Taylor expansion, the loss function can be simplified as:

$$\mathcal{L}_{p2n} \approx 4\sigma^2 \left\| \frac{\partial \mathcal{F}_\theta(x)}{\partial x} \cdot n \right\|^2. \quad (16)$$

where $\frac{\partial \mathcal{F}_\theta(x)}{\partial x} \cdot n$ reflects the sensitivity of the neural network \mathcal{F}_θ to noise. The derivation of Eq. (16) is provided in the supplementary material.

Through consistency loss L_{p2n} , we optimize the network \mathcal{F}_θ such that $\frac{\partial \mathcal{F}_\theta(x)}{\partial x} \cdot n$ is optimized to drive towards zero. When $\frac{\partial \mathcal{F}_\theta(x)}{\partial x} \cdot n \rightarrow 0$, the output $\mathcal{F}_\theta(y)$ tends to:

$$\mathcal{F}_\theta(y) = \mathcal{F}_\theta(x + n), \quad (17)$$

$$= \mathcal{F}_\theta(x) + \frac{\partial \mathcal{F}_\theta(x)}{\partial x} \cdot n + \mathcal{O}(n^2), \quad (18)$$

$$\approx \mathcal{F}_\theta(x) \quad (19)$$

Ideally, the neural network \mathcal{F}_θ has learned image priors, the model output $\mathcal{F}_\theta(x)$ matches the clean signal x and we have $\mathcal{F}_\theta(x) = x$. Thus, the ultimate goal achieves:

$$\mathcal{F}_\theta(y) \approx x. \quad (20)$$

In summary, the neural network \mathcal{F}_θ gradually learns to denoise the noisy image y effectively.

4. Experiments

In this section, we first introduce the experimental settings in Section 4.1. After that, we demonstrate the performance

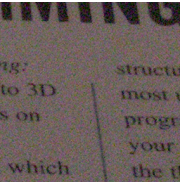
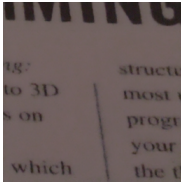
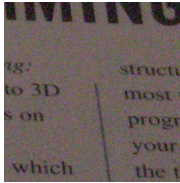
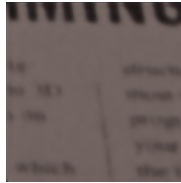
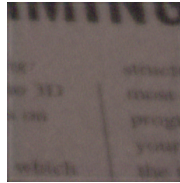
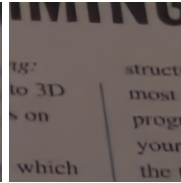
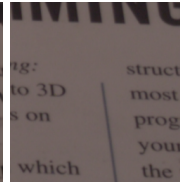
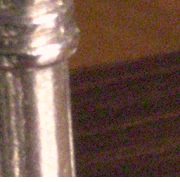
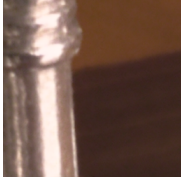
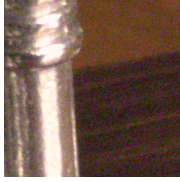
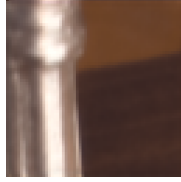
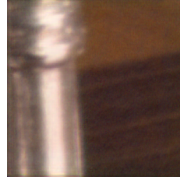
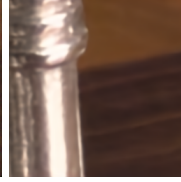
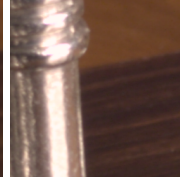







Noisy	ScoreDVI [9]	ZS-N2N [25]	MASH [11]	ATBSN-single [8]	P2N (Ours)	Reference
						
25.54 / 0.432	36.17 / 0.958	27.10 / 0.529	32.48 / 0.878	30.23 / 0.795	37.67 / 0.970	PSNR / SSIM
						
24.99 / 0.479	34.32 / 0.930	26.63 / 0.556	30.64 / 0.881	27.12 / 0.799	35.14 / 0.950	PSNR / SSIM
						
24.99 / 0.566	32.12 / 0.848	26.52 / 0.638	31.23 / 0.791	28.22 / 0.643	32.95 / 0.887	PSNR / SSIM

Figure 6. **Qualitative comparisons** of P2N against other self-supervised single image denoising methods in SIDD validation dataset. The denoised results of ScoreDVI are always flaky, with discontinuous lines and loss of texture. ZS-N2N does not completely denoise the images. MASH and ATBSN-single tend to either meet aliasing effect or blur the details. In summary, other methods meet aliasing effects and loss of texture, while Positive2Negative achieves both detailed texture preservation and comprehensive noise removal. In the figure, P2N represents Positive2Negative.

and comparisons with other methods in Section 4.2. Finally, we conduct a detailed ablation study in Section 4.3.

4.1. Settings

In this section, we briefly introduce the experimental settings and details. More details can be found in the supplementary materials.

Datasets details. Following previous methods [9, 11], we evaluate the proposed paradigm on the widely-used datasets in self-supervised single image denoising: the SIDD validation dataset [1], the SIDD benchmark dataset [1], CC [27], PolyU [46] and FMDD [50]. The SIDD, PolyU and CC datasets consist of natural sRGB images, while the FMDD dataset consists of fluorescence microscopy images.

Implementation details. Following the default settings of self-supervised single image denoising methods [9, 11, 20, 37], we employ the same neural network architecture as Noise2Noise [20] and MASH [11] and initialize the neural network parameters with those pre-trained on Gaussian noise [9, 52]. For training details, we employ AdamW [24] optimizer with a learning rate of 0.0001 and set scale parameter $\sigma = 0.75$, for all the experiments. No image enhancement techniques are applied.

Compared methods. Following previous methods [9, 11, 22], we mainly compare with self-supervised single image

denoising methods. In addition, we also present the results of noisy dataset based self-supervised and supervised image denoising methods only as a reference comparison. All the results of the comparison methods are sourced from previous work [9, 11, 22] or evaluated by ourselves.

4.2. Comparisons

In this section, we demonstrate the performance of Positive2Negative and compare Positive2Negative with other methods both quantitatively and qualitatively.

Quantitative comparisons. The quantitative comparisons are described in Table 1. Previous self-supervised single image denoising methods have shown varying performance across different datasets, but Positive2Negative consistently achieves better results. In fact, Positive2Negative even outperforms some dataset-based and supervised methods. Notably, in the online evaluation of the SIDD benchmark dataset, we achieve an improvement of over 0.4 dB.

Qualitative comparisons. The qualitative comparisons are described in Figure 6. Clearly, the Positive2Negative paradigm achieves significant qualitative improvements by either enhancing details or effectively reducing noise. In contrast, other methods face limitations in both detail enhancement and noise removal due to the difficulty in learning denoising, resulting from the information-lossy barrier.

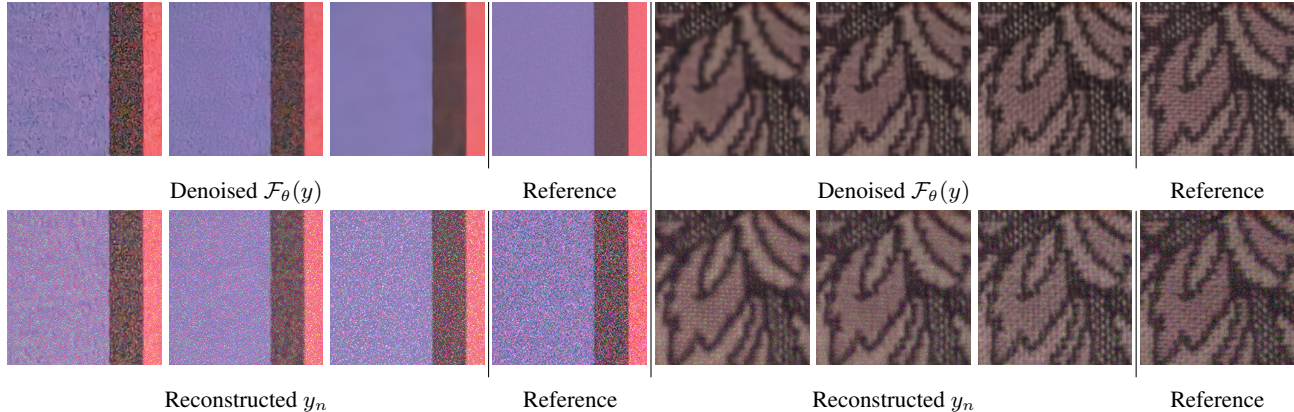


Figure 7. **Visual results** of the training process. The top row shows the denoised results, while the bottom row displays the reconstructed negative noisy images in the training process. On the far right of each set is the reference image. The denoised image and reconstructed noisy image gradually become more like the reference images.

Table 2. **Ablation of components.** Each step is crucial for Positive2Negative. N2N and N2V represent Noise2Noise and Noise2Void, respectively.

Method	CC [27]		SIDD [1]	
	PSNR	SSIM	PSNR	SSIM
Baseline	35.40	0.980	33.50	0.849
RDC+N2N	34.08	0.902	25.42	0.487
RDC+N2V	33.79	0.895	24.51	0.408
N2N+DCS	17.55	0.731	24.20	0.855
N2V+DCS	14.14	0.527	22.30	0.773
RDC+DCS	37.92	0.987	35.24	0.928

More additional visual comparisons can be found in the supplementary materials.

4.3. Ablations

In this section, we first present the training process in Section 4.3.1. Then, we conduct ablation studies on the components and hyperparameters in Section 4.3.2 and Section 4.3.3, respectively.

4.3.1. Ablation of training

We present visual results of the training process to illustrate the effectiveness of our Positive2Negative paradigm. As shown in Figure 7, our method learns robust denoising for images with various levels of noise, ensuring both detailed texture preservation and comprehensive noise removal. Throughout the training process, the denoised images and the reconstructed negative noisy images gradually converge towards their respective references.

Table 3. **Ablation of hyperparameters.** The scale parameter is the only hyperparameter and is very robust. We fix the scale parameter $\sigma = 0.75$ for all the experiments.

Method	CC [27]		SIDD [1]	
	PSNR	SSIM	PSNR	SSIM
Fixed	37.67	0.985	35.24	0.932
$\sigma = 0.25$	37.90	0.989	35.29	0.933
$\sigma = 0.50$	37.90	0.989	35.30	0.931
$\sigma = 0.75$	37.92	0.987	35.24	0.928
$\sigma = 1.00$	37.87	0.987	35.11	0.924

4.3.2. Ablation of components

We evaluate the effectiveness of each component of the Positive2Negative paradigm on the CC and SIDD datasets. RDC constructs precise training data and DCS trains robust denoising neural networks. Both RDC and DCS are crucial for Positive2Negative. Replacing either component would result in a decline in performance, as shown in Table 2.

4.3.3. Ablation of hyperparameters

It’s worth noting that the Positive2Negative paradigm requires no hyperparameter tuning. Throughout the entire training process, the only adjustable parameter is the scale parameter σ . We set $\sigma = 0.75$ for all experiments. In this section, we demonstrate that the Positive2Negative paradigm is robust to the scale parameter.

As shown in Table 3, the performance remains consistent with nearly identical results for σ values ranging from 0.25 to 0.75. The scale parameter σ introduces a dynamic and wide range of noise levels, while the “Fixed” setting corresponds to $\sigma = 0$.

Table 4. **Discussion of distributions.** Noise generally has a zero-mean. Even if there is a deviation, the deviation is always slight, which the $\|\cdot\|_{2 \rightarrow 1.5}$ norm can effectively handle.

Dataset	$\ \cdot\ _0$	$\ \cdot\ _1$	$\ \cdot\ _2$	$\ \cdot\ _{2 \rightarrow 1.5}$
CC [27]	34.89	37.81	37.87	37.92
PolyU [46]	37.88	38.02	38.20	38.20

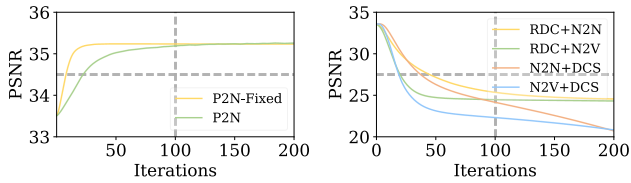


Figure 8. **Convergence comparisons.** P2N converges quickly and remains highly stable after convergence. The P2N-Fixed version (where $\sigma = 0.00$), in particular, even achieves rapid convergence in approximately 10 iterations. P2N represents Positive2Negative.

5. Discussions

In this section, we discuss several issues that may be of concern. More discussions could be found in the supplementary materials.

5.1. Distribution

In real-world datasets, noise is typically centered around zero mean [16, 20], with only slight fluctuations. Positive2Negative does not require the noise distribution to be strictly zero-mean, as the loss function could handle slight fluctuations [20]. For datasets with nearly zero-mean, such as the PolyU [46], the performance of the $\|\cdot\|_{2 \rightarrow 1.5}$ norm and the $\|\cdot\|_2$ norm are generally similar. For datasets where the noise exhibits slight deviations, such as the CC [27], the $\|\cdot\|_{2 \rightarrow 1.5}$ norm can outperform the $\|\cdot\|_2$ norm as demonstrated in Table 4. The small PSNR increase also indicates that the deviation between the mean and zero is slight.

5.2. Convergence

We present the PSNR variation over iterations in Figure 8. Around the 100th iteration, the Positive2Negative paradigm converges and shows minimal fluctuations thereafter, indicating no signs of overfitting or collapse. Additionally, it is worth noting that the constructed data by RDC is unsuitable for Noise2Noise and Noise2Void. This is mainly because the noise in constructed images by RDC is correlated, which would quickly collapse the training processes of the other two methods.

5.3. Efficiency

For self-supervised single image denoising methods, one crucial factor is speed, necessitating training on each noisy image individually. The training iterations, parameters,

Table 5. **Efficiency comparisons** under input images with dimensions of $256 \times 256 \times 3$. With similar parameters and FLOPs, P2N requires the fewest training iterations. P2N converges rapidly, and the P2N-Fixed version (where $\sigma = 0.00$) converges even just within 20 iterations. P2N represents Positive2Negative.

Method	Iterations	Params (M)	FLOPs (G)
N2N [20]	-	0.70	18.7
B2U [37]	-	1.10	18.7
Self2Self [33]	450000	1.00	9.6
R2R [31]	8000	0.56	36.7
ScoreDVI [9]	1200	13.5	37.9
MASH [11]	2400	0.99	11.4
P2N-Fixed	<20	0.99	11.4
P2N	<100	0.99	11.4

and computational efforts are detailed in Table 5. Historically, many methods required training a lot of iterations per single image. In contrast, our paradigm achieves about a $10 \times \sim 50 \times$ speedup compared to the existing solution. Specifically, we just need a few minutes or a few hours to finish the training for the whole SIDD dataset.

5.4. Comparison with Noise2Noise and Noise2Void

Positive2Negative, a concise yet highly effective paradigm, also presents an elegant solution with distinct differences compared to Noise2Noise and Noise2Void.

Firstly, for the constructed data, the synthetic data constructed by Positive2Negative breaks the information-lossy barrier of Noise2Noise and Noise2Void. Secondly, for the supervision strategy, Positive2Negative enforces consistency between denoised results, whereas Noise2Noise and Noise2Void supervise the consistency between a denoised result and a noisy image. Thirdly, from the assumption perspective, Noise2Noise, Noise2Void, and Positive2Negative all have theoretical guarantees, while Noise2Noise and Noise2Void operate under more restrictive assumptions. Noise2Noise requires two independent noisy images, while Noise2Void assumes that the noise is spatially correlated.

The above differences are the reason for the collapse when training Noise2Noise and Noise2Void with the constructed data from Positive2Negative, as shown in Figure 8.

6. Conclusion

In this paper, we propose a self-supervised single image denoising paradigm, Positive2Negative, to break information-lossy barrier. Specifically, Positive2Negative includes two steps: RDC and DCS. Positive2Negative achieves SOTA performance compared to existing methods across various public benchmarks.

References

- [1] Abdelrahman Abdelhamed, Stephen Lin, and Michael S. Brown. A high-quality denoising dataset for smartphone cameras. In *Proceedings of the IEEE/CVF Conference on Computer Vision and Pattern Recognition (CVPR)*, pages 1692–1700, 2018. [1](#), [5](#), [6](#), [7](#)
- [2] Joshua Batson and Loic Royer. Noise2Self: Blind denoising by self-supervision. In *International Conference on Machine Learning (ICML)*, pages 524–533, 2019. [2](#)
- [3] Chinmay Belthangady and Loic A Royer. Applications, promises, and pitfalls of deep learning for fluorescence image reconstruction. In *Nature methods*, pages 1215–1225, 2019. [1](#)
- [4] Tim Brooks, Ben Mildenhall, Tianfan Xue, Jiawen Chen, Dillon Sharlet, and Jonathan T Barron. Unprocessing images for learned raw denoising. In *Proceedings of the IEEE/CVF Conference on Computer Vision and Pattern Recognition (CVPR)*, pages 11036–11045, 2019. [5](#)
- [5] Jaeseok Byun, Sungmin Cha, and Taesup Moon. Fbi-denoiser: Fast blind image denoiser for poisson-gaussian noise. In *Proceedings of the IEEE/CVF Conference on Computer Vision and Pattern Recognition (CVPR)*, pages 5768–5777, 2021. [3](#)
- [6] Haoyu Chen, Jinjin Gu, Yihao Liu, Salma Abdel Magid, Chao Dong, Qiong Wang, Hanspeter Pfister, and Lei Zhu. Masked image training for generalizable deep image denoising. In *Proceedings of the IEEE/CVF Conference on Computer Vision and Pattern Recognition (CVPR)*, pages 1692–1703, 2023. [5](#)
- [7] Liangyu Chen, Xiaojie Chu, Xiangyu Zhang, and Jian Sun. Simple baselines for image restoration. In *European Conference on Computer Vision (ECCV)*, pages 17–33, 2022. [1](#)
- [8] Shiyan Chen, Jiyuan Zhang, Zhaofei Yu, and Tiejun Huang. Exploring efficient asymmetric blind-spots for self-supervised denoising in real-world scenarios. In *Proceedings of the IEEE/CVF Conference on Computer Vision and Pattern Recognition (CVPR)*, pages 2814–2823, 2024. [1](#), [2](#), [3](#), [5](#), [6](#)
- [9] Jun Cheng, Tao Liu, and Shan Tan. Score priors guided deep variational inference for unsupervised real-world single image denoising. In *Proceedings of the IEEE/CVF Conference on Computer Vision and Pattern Recognition (CVPR)*, pages 12937–12948, 2023. [1](#), [3](#), [5](#), [6](#), [8](#)
- [10] Jun Cheng, Dong Liang, and Shan Tan. Transfer clip for generalizable image denoising. In *Proceedings of the IEEE/CVF Conference on Computer Vision and Pattern Recognition (CVPR)*, pages 25974–25984, 2024. [5](#)
- [11] Hamadi Chihaoui and Paolo Favaro. Masked and shuffled blind spot denoising for real-world images. In *Proceedings of the IEEE/CVF Conference on Computer Vision and Pattern Recognition (CVPR)*, pages 3025–3034, 2024. [1](#), [2](#), [3](#), [5](#), [6](#), [8](#)
- [12] Samuel W Hasinoff, Dillon Sharlet, Ryan Geiss, Andrew Adams, Jonathan T Barron, Florian Kainz, Jiawen Chen, and Marc Levoy. Burst photography for high dynamic range and low-light imaging on mobile cameras. In *ACM Transactions on Graphics (ToG)*, pages 1–12, 2016. [1](#)
- [13] Tao Huang, Songjiang Li, Xu Jia, Huchuan Lu, and Jianzhuang Liu. Neighbor2Neighbor: Self-supervised denoising from single noisy images. In *Proceedings of the IEEE/CVF Conference on Computer Vision and Pattern Recognition (CVPR)*, pages 14781–14790, 2021. [1](#), [2](#)
- [14] Yeong Il Jang, Keuntek Lee, Gu Yong Park, Seyun Kim, and Nam Ik Cho. Self-supervised image denoising with down-sampled invariance loss and conditional blind-spot network. In *Proceedings of the IEEE/CVF International Conference on Computer Vision (ICCV)*, pages 12196–12205, 2023. [3](#)
- [15] Kwanyoung Kim, Taesung Kwon, and Jong Chul Ye. Noise distribution adaptive self-supervised image denoising using tweedie distribution and score matching. In *Proceedings of the IEEE/CVF Conference on Computer Vision and Pattern Recognition (CVPR)*, pages 1998–2006, 2022. [3](#)
- [16] Alexander Krull, Tim-Oliver Buchholz, and Florian Jug. Noise2void: Learning denoising from single noisy images. In *Proceedings of the IEEE/CVF Conference on Computer Vision and Pattern Recognition (CVPR)*, pages 2129–2137, 2019. [1](#), [2](#), [3](#), [5](#), [8](#)
- [17] Alexander Krull, Tomáš Vičar, Mangal Prakash, Manan Lalit, and Florian Jug. Probabilistic noise2void: Unsupervised content-aware denoising. In *Frontiers in Computer Science*, pages 2–5, 2020. [2](#)
- [18] Samuli Laine, Tero Karras, Jaakko Lehtinen, and Timo Aila. High-quality self-supervised deep image denoising. In *Proceedings of International Conference on Neural Information Processing Systems (NeurIPS)*, pages 6970–6980, 2019. [2](#)
- [19] Wooseok Lee, Sanghyun Son, and Kyoung Mu Lee. AP-BSN: Self-supervised denoising for real-world images via asymmetric pd and blind-spot network. In *Proceedings of the IEEE/CVF Conference on Computer Vision and Pattern Recognition (CVPR)*, pages 17725–17734, 2022. [2](#), [3](#), [5](#)
- [20] Jaakko Lehtinen, Jacob Munkberg, Jon Hasselgren, Samuli Laine, Tero Karras, Miika Aittala, and Timo Aila. Noise2Noise: Learning image restoration without clean data. In *International Conference on Machine Learning (ICML)*, pages 4620–4631, 2018. [1](#), [2](#), [3](#), [4](#), [6](#), [8](#)
- [21] Junyi Li, Zhilu Zhang, Xiaoyu Liu, Chaoyu Feng, Xiaotao Wang, Lei Lei, and Wangmeng Zuo. Spatially adaptive self-supervised learning for real-world image denoising. In *Proceedings of the IEEE/CVF Conference on Computer Vision and Pattern Recognition (CVPR)*, pages 9914–9924, 2023. [3](#)
- [22] Tong Li, Hansen Feng, Lizhi Wang, Zhiwei Xiong, and Hua Huang. Stimulating the diffusion model for image denoising via adaptive embedding and ensembling. In *IEEE Transactions on Pattern Analysis and Machine Intelligence (TPAMI)*, pages 8240–8257, 2024. [1](#), [6](#)
- [23] Xinyang Li, Yixin Li, Yiliang Zhou, Jiamin Wu, Zhifeng Zhao, Jiaqi Fan, Fei Deng, Zhaofa Wu, Guihua Xiao, Jing He, Yuanlong Zhang, Guoxun Zhang, Xiaowan Hu, Zhang Yi Chen, Xingye and, Hui Qiao, Hao Xie, Yulong Li, Haoqian Wang, Lu Fang, and Qionghai Dai. Real-time denoising enables high-sensitivity fluorescence time-lapse imaging beyond the shot-noise limit. In *Nature Biotechnology*, pages 282–292, 2023. [1](#)
- [24] Ilya Loshchilov, Frank Hutter, et al. Fixing weight decay

- regularization in adam. In *arXiv preprint arXiv:1711.05101*, pages 1–10, 2017. [6](#)
- [25] Youssef Mansour and Reinhard Heckel. Zero-Shot Noise2Noise: Efficient image denoising without any data. In *Proceedings of the IEEE/CVF Conference on Computer Vision and Pattern Recognition (CVPR)*, pages 14018–14027, 2023. [1](#), [2](#), [3](#), [5](#), [6](#)
- [26] Nick Moran, Dan Schmidt, Yu Zhong, and Patrick Coady. Noisier2Noise: Learning to denoise from unpaired noisy data. In *Proceedings of the IEEE/CVF Conference on Computer Vision and Pattern Recognition (CVPR)*, pages 12064–12072, 2020. [1](#), [2](#)
- [27] Seonghyeon Nam, Youngbae Hwang, Yasuyuki Matsushita, and Seon Joo Kim. A holistic approach to cross-channel image noise modeling and its application to image denoising. In *Proceedings of the IEEE/CVF Conference on Computer Vision and Pattern Recognition (CVPR)*, pages 1683–1691, 2016. [5](#), [6](#), [7](#), [8](#)
- [28] Reyhaneh Neshatavar, Mohsen Yavartanoo, Sanghyun Son, and Kyoung Mu Lee. CVF-SID: Cyclic multi-variate function for self-supervised image denoising by disentangling noise from image. In *Proceedings of the IEEE/CVF Conference on Computer Vision and Pattern Recognition*, pages 17583–17591, 2022. [3](#), [5](#)
- [29] Harry Nyquist. Certain topics in telegraph transmission theory. In *Transactions of the American Institute of Electrical Engineers*, pages 617–644, 1928. [1](#), [2](#)
- [30] Yizhong Pan, Xiao Liu, Xiangyu Liao, Yuanzhouhan Cao, and Chao Ren. Random sub-samples generation for self-supervised real image denoising. In *Proceedings of the IEEE/CVF International Conference on Computer Vision (ICCV)*, pages 12150–12159, 2023. [2](#), [3](#)
- [31] Tongyao Pang, Huan Zheng, Yuhui Quan, and Hui Ji. Recorrupted-to-Recorrupted: Unsupervised deep learning for image denoising. In *Proceedings of the IEEE/CVF Conference on Computer Vision and Pattern Recognition (CVPR)*, pages 2043–2052, 2021. [1](#), [2](#), [3](#), [5](#), [8](#)
- [32] Tobias Plotz and Stefan Roth. Benchmarking denoising algorithms with real photographs. In *Proceedings of the IEEE/CVF Conference on Computer Vision and Pattern Recognition (CVPR)*, pages 1586–1595, 2017. [1](#)
- [33] Yuhui Quan, Mingqin Chen, Tongyao Pang, and Hui Ji. Self2Self with dropout: Learning self-supervised denoising from single image. In *Proceedings of the IEEE/CVF Conference on Computer Vision and Pattern Recognition (CVPR)*, pages 1890–1898, 2020. [3](#), [5](#), [8](#)
- [34] Claude Elwood Shannon. A mathematical theory of communication. In *The Bell system technical journal*, pages 379–423, 1948. [1](#), [2](#)
- [35] Andrea Vedaldi Ulyanov Dmitry and Victor Lempitsky. Deep image prior. In *Proceedings of the IEEE/CVF Conference on Computer Vision and Pattern Recognition (CVPR)*, pages 9446–9454, 2018. [3](#), [5](#)
- [36] Yuzhi Wang, Haibin Huang, Qin Xu, Jiaming Liu, Yiqun Liu, and Jue Wang. Practical deep raw image denoising on mobile devices. In *European Conference on Computer Vision (ECCV)*, pages 1–16, 2020. [1](#)
- [37] Zejin Wang, Jiazheng Liu, Guoqing Li, and Hua Han. Blind2Unblind: Self-supervised image denoising with visible blind spots. In *Proceedings of the IEEE/CVF Conference on Computer Vision and Pattern Recognition (CVPR)*, pages 2027–2036, 2022. [2](#), [6](#), [8](#)
- [38] Zichun Wang, Ying Fu, Ji Liu, and Yulun Zhang. LG-BPN: Local and global blind-patch network for self-supervised real-world denoising. In *Proceedings of the IEEE/CVF Conference on Computer Vision and Pattern Recognition (CVPR)*, pages 18156–18165, 2023. [2](#), [3](#)
- [39] Kaixuan Wei, Ying Fu, Yinqiang Zheng, and Jiaolong Yang. Physics-based noise modeling for extreme low-light photography. In *IEEE Transactions on Pattern Analysis and Machine Intelligence (TPAMI)*, pages 8520–8537, 2021. [1](#)
- [40] Martin Weigert, Uwe Schmidt, Tobias Boothe, Andreas Müller, Alexandr Dibrov, Akanksha Jain, Benjamin Wilhelm, Deborah Schmidt, Coleman Broaddus, Siân Culley, et al. Content-aware image restoration: pushing the limits of fluorescence microscopy. In *Nature methods*, pages 1090–1097, 2018. [1](#)
- [41] Halbert White. Connectionist nonparametric regression: Multilayer feedforward networks can learn arbitrary mappings. In *Neural networks*, pages 535–549, 1990. [2](#)
- [42] David Wu, Damian Tan, Marilyn Baird, John DeCampo, Chris White, and Hong Ren Wu. Perceptually lossless medical image coding. In *IEEE Transactions on Medical Imaging*, pages 335–344, 2006. [2](#)
- [43] Hong Ren Wu, Weisi Lin, and Lina J. Karam. An overview of perceptual processing for digital pictures. In *IEEE International Conference on Multimedia and Expo Workshops*, pages 113–120, 2012. [2](#)
- [44] Xiaohe Wu, Ming Liu, Yue Cao, Dongwei Ren, and Wangmeng Zuo. Unpaired learning of deep image denoising. In *European Conference on Computer Vision (ECCV)*, pages 352–368, 2020. [3](#)
- [45] Yaochen Xie, Zhengyang Wang, and Shuiwang Ji. Noise2same: Optimizing a self-supervised bound for image denoising. In *Advances in Neural Information Processing Systems*, pages 20320–20330, 2020. [2](#)
- [46] Jun Xu, Hui Li, Zhetong Liang, David Zhang, and Lei Zhang. Real-world noisy image denoising: A new benchmark. In *arXiv preprint arXiv:1804.02603*, pages 1–13, 2018. [5](#), [6](#), [8](#)
- [47] Jun Xu, Yuan Huang, Ming-Ming Cheng, Li Liu, Fan Zhu, Zhou Xu, and Ling Shao. Noisy-as-Clean: Learning self-supervised denoising from corrupted image. In *IEEE Transactions on Image Processing (TIP)*, pages 9316–9329, 2020. [2](#)
- [48] Syed Waqas Zamir, Aditya Arora, Salman Khan, Munawar Hayat, Fahad Shahbaz Khan, and Ming-Hsuan Yang. Restormer: Efficient transformer for high-resolution image restoration. In *Proceedings of the IEEE/CVF Conference on Computer Vision and Pattern Recognition (CVPR)*, pages 5728–5739, 2022. [1](#)
- [49] Dan Zhang, Fangfang Zhou, Yuwen Jiang, and Zhengming Fu. Mm-bsn: Self-supervised image denoising for real-world with multi-mask based on blind-spot network. In *Proceed-*

- ings of the IEEE/CVF Conference on Computer Vision and Pattern Recognition Workshops*, pages 4189–4198, 2023. [2](#)
- [50] Yide Zhang, Yinhao Zhu, Evan Nichols, Qingfei Wang, Siyuan Zhang, Cody Smith, and Scott Howard. A poisson-gaussian denoising dataset with real fluorescence microscopy images. In *Proceedings of the IEEE/CVF Conference on Computer Vision and Pattern Recognition (CVPR)*, pages 11710–11718, 2019. [5](#), [6](#)
- [51] Yi Zhang, Dasong Li, Ka Lung Law, Xiaogang Wang, Hongwei Qin, and Hongsheng Li. IDR: Self-supervised image denoising via iterative data refinement. In *Proceedings of the IEEE/CVF Conference on Computer Vision and Pattern Recognition (CVPR)*, pages 2098–2107, 2022. [2](#)
- [52] Dihan Zheng, Sia Huat Tan, Xiaowen Zhang, Zuoqiang Shi, Kaisheng Ma, and Chenglong Bao. An unsupervised deep learning approach for real-world image denoising. In *International Conference on Learning Representations (ICLR)*, pages 1–9, 2020. [5](#), [6](#)
- [53] Dihan Zheng, Xiaowen Zhang, Kaisheng Ma, and Chenglong Bao. Learn from unpaired data for image restoration: A variational bayes approach. In *IEEE Transactions on Pattern Analysis and Machine Intelligence (TPAMI)*, pages 5889–5903, 2022. [3](#), [5](#)
- [54] Yuqian Zhou, Jianbo Jiao, Haibin Huang, Yang Wang, Jue Wang, Honghui Shi, and Thomas Huang. When awgn-based denoiser meets real noises. In *Proceedings of the AAAI Conference on Artificial Intelligence (AAAI)*, pages 13074–13081, 2020. [3](#), [5](#)
- [55] Yunhao Zou, Chenggang Yan, and Ying Fu. Iterative denoiser and noise estimator for self-supervised image denoising. In *Proceedings of the IEEE/CVF Conference on Computer Vision and Pattern Recognition (CVPR)*, pages 13265–13274, 2023. [2](#)